Journal of Nuclear Materials 409 (2011) 40–46

Contents lists available at ScienceDirect

Journal of Nuclear Materials

journal homepage: www.elsevier.com/locate/jnucmat

Dynamic Young's moduli of tungsten and tantalum at high temperature and stress ☆

G.P. Škoro [a,*], J.R.J. Bennett [b], T.R. Edgecock [b,c], S.A. Gray [b], A.J. McFarland [b], C.N. Booth [a], K.J. Rodgers [b], J.J. Back [d]

[a] Department of Physics and Astronomy, University of Sheffield, Sheffield S3 7RH, UK
[b] STFC, Rutherford Appleton Laboratory, Chilton, Didcot, Oxon OX11 0QX, UK
[c] University of Huddersfield, Queensgate, Huddersfield HD1 3DH, UK
[d] Department of Physics, University of Warwick, Coventry CV4 7AL, UK

ARTICLE INFO

Article history:
Received 1 November 2010
Accepted 17 December 2010
Available online 25 December 2010

ABSTRACT

Recently reported results of the long lifetime of the tungsten samples under high temperature and high stress conditions expected in the Neutrino Factory target have strengthened the case for a solid target option for the Neutrino Factory. In order to study in more detail the behaviour of the material properties of tungsten, a dynamic method has been used for measurement of Young's modulus at high stress, high-strain-rates (>1000 s^{-1}) and very high temperatures (up to 2650 °C). The method is based on measurements of the surface vibration of thin wires, stressed by a pulsed current, using a Laser Doppler Vibrometer. The measured characteristic frequencies under the thermal excitation have been used to obtain Young's modulus as a function of applied stress and temperature. The same procedure has been used to measure Young's modulus of tantalum up to 2500 °C.

1. Introduction

The answer to the fundamental question of the role of neutrinos in the creation of our universe requires precise measurements of the parameters governing neutrino oscillations. The precision required for these measurements demands a new facility, and current simulations suggest this facility should be a Neutrino Factory [1]. The target system at the Neutrino Factory must generate the maximum number of pions from an intense nanosecond-long pulsed proton beam. Several target designs have been explored by various collaborations and laboratories around the world. The UK programme of high power target developments for a Neutrino Factory [2] is centred on the study of high atomic number (Z) solid materials (tantalum and tungsten).

The beam power at the Neutrino Factory will be 4 MW and around 700 kW will be deposited in the target so the magnitude of thermal stress is the main issue for solid targets [2]. To test the response of the targets to this stress, a fast, high current pulse generating the same stress was passed through a thin wire made of the candidate material. Extensive tests have been performed to determine the number of current pulses before the wire visibly deteriorates [2,3]. These measurements are made at temperatures up to 2000 K. The stress on the wire is calculated and compared to the stress expected in the target using the finite element code LS-DYNA [4]. It has been found that tantalum is too weak to sustain prolonged stress at these temperatures but a tungsten wire has reached over 26 million pulses (equivalent to 10 years of operation at the Neutrino Factory) at the stress expected in the target [2].

Typically a plot of stress versus strain for a metal will show a linear rise of strain with steadily increasing applied stress (the slope gives Young's modulus) [5]. At some point the stress becomes so high that the strain starts to increase more rapidly leading to the material failure. It was of interest to examine the behaviour of the test wires at high stress for any similar behaviour, resulting in a measurement of the Young's modulus as a function of stress and temperature with the dynamic method described here.

The rest of the paper is organized as follows. Section 2 describes the experimental setup. The detailed description of the method, analysis techniques and results are given in Sections 3.1 and 3.2 for tungsten and the results for tantalum in Section 3.3. Discussion of the results are presented in Section 4, followed by the summary in Section 5.

2. Experimental setup

The experiment is shown in Fig. 1. A thin wire is necessary to allow the current to diffuse into the centre of the wire in a sufficiently short time to generate sufficient thermal stress. For tungsten, the wire cannot be greater than ~1 mm in diameter.

The tungsten and tantalum wires with diameters from 0.38 mm to 1 mm have been made by standard powder metallurgy methods-pressing, sintering, forging and finally drawing. The purity of the tungsten wires used in the tests was 99.9+% . The purity of

☆ Work supported by Science and Technology Facilities Council (UK).
* Corresponding author.
E-mail address: g.skoro@sheffield.ac.uk (G.P. Škoro).

0022-3115/$ - see front matter © 2010 Elsevier B.V. All rights reserved.
doi:10.1016/j.jnucmat.2010.12.222

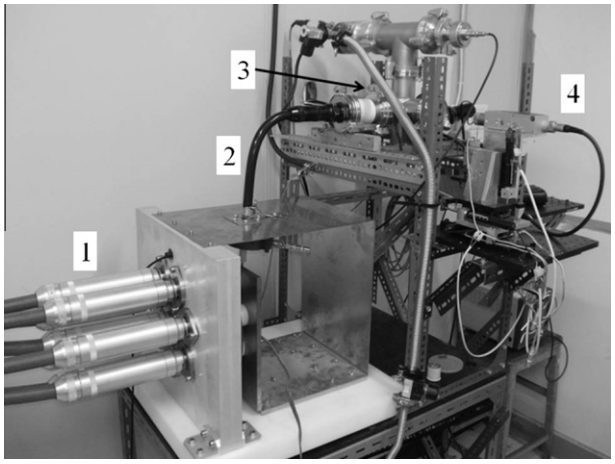

Fig. 1. The experimental setup. Coaxial cables (1) carry the current pulse from the power supply (not shown) and they are combined into a single cable (2) which is connected to the test wire. The wire is supported in a vacuum chamber (3) and its oscillations are measured by the Laser Doppler Vibrometer (4).

the tantalum wires was 99.9%. The tungsten wires have been additionally stress relieved at about 400 °C.

To generate a current pulse a power supply for the ISIS [6] kicker magnets has been used, supplying a maximum of 60 kV and 9200 A at up to 50 Hz in a pulse which rises in 100 ns and is ~800 ns long. Coaxial cables of 100 m length (left hand side of Fig. 1) carry the current pulse from the power supply and they are combined into a single cable which is connected to the test wire. The wires, of 3–10 cm length, are supported in a vacuum chamber to avoid oxidation (Figs. 1 and 2a). One end of the wire is firmly clamped, while the other end is allowed to expand freely through a pair of graphite conductors that lightly clamp the wire (see Fig. 2b). The movements of the test wire during the pulsing is measured by a laser Doppler vibrometer (LDV). A single point LDV from Polytec [7] with the optical sensor head OFV-534 connected to the OFV-5000 vibrometer controller was used to measure the longitudinal and radial velocity and displacements of the tantalum and tungsten wires. Three different decoder units have been used to cover the complete range of amplitudes and frequencies of the wire vibrations:

- the VD-02 velocity decoder with a 10 m/s maximum velocity and 1.5 MHz upper frequency limit;
- the DD-300 displacement decoder with the 24 MHz upper frequency limit and an amplitude range from −75 to +75 nm;
- and the VD-05 velocity decoder with a 2.5 m/s maximum velocity and 10 MHz upper frequency limit.

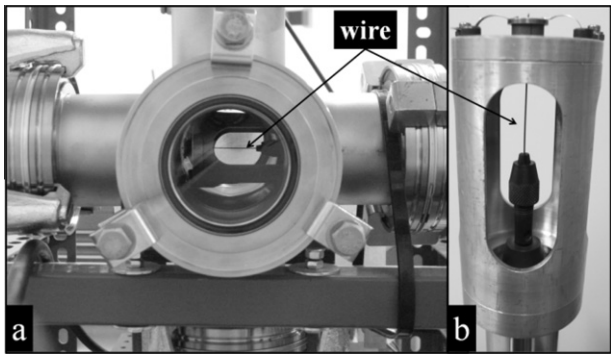

Fig. 2. Photograph of a 0.75 mm diameter tungsten wire during current pulse tests (a) and illustration of wire clamping (b).

2.1. Temperature measurements

The wire is operated at temperatures from 300 to 2900 K by adjusting the pulse repetition rate. The wire temperature is measured by a manually operated optical pyrometer. The optical pyrometer reading must be corrected for the emissivity of the sample. As the emissivity strongly depends on its surface roughness it has been necessary to measure the properties of the surfaces of our test wires. Measurements of surface roughness and precise determination of wire diameters were performed at the Metrology Facility at RAL and the results for the tungsten samples are summarized in Table 1.

Measured values of surface roughness have been used to obtain the corresponding emissivity and temperature corrections by scaling up the emissivity versus temperature result for a tungsten sample with a perfectly smooth surface [8]. A similar procedure has been applied for the tantalum samples. All temperatures reported in this paper have been corrected for the measured emissivity.

3. Results

3.1. Young's modulus of tungsten at room temperature

The dotted line in Fig. 3 shows the measured longitudinal velocity of a 4.6 cm long tungsten wire. In this case, the wire has been heated by a single current pulse with peak voltage of 50 kV, and peak current of 7.75 kA. The full line shows the result of corresponding LS-DYNA simulations [9]. The time scale in Fig. 3 starts at $t < 0$ in order to illustrate a relatively low level of noise of the LDV. At $t = 0$ the current pulse begins and longitudinal expansion and contraction of the wire can be clearly seen. The movement of the end of the wire is relatively complicated so additional processing is needed in order to explain all the effects.

A short routine has been written in MATLAB [10] for the fast Fourier transform (FFT) analysis of the LDV signals. The result of the frequency analysis of the longitudinal motion taken from Fig. 3 is shown in Fig. 4. The characteristic signature in the FFT spectrum is a fundamental frequency and a set of higher harmonics. The fundamental frequency, f_0, and higher harmonics, f_n, depend on material properties and wire length:

$$f_n = (2n+1)\frac{c}{4l} = \frac{(2n+1)}{4l}\sqrt{\frac{E}{\rho}}, \tag{1}$$

where l is the length of the wire, c is the speed of sound, E is Young's modulus and ρ is the density of the material. At least eight harmonics can be clearly seen in Fig. 4 (only six of them have been highlighted) and these can be used to precisely extract the value of Young's modulus for tungsten at room temperature.

Combining the measured value of the fundamental frequency $f_0 = (24.3 \pm 0.3)$ kHz and the value of the density of tungsten at room temperature from the temperature-dependent parametrization [11]:

$$\rho = 19.3027 + 2.3786 \times 10^{-4} \cdot T - 2.244 \times 10^{-8} \cdot T^2, \tag{2}$$

where ρ is given in (g/cm^3) and temperature in (°C), we have obtained: $E = (386 \pm 5)$ GPa.

Table 1
Surface roughness of the tungsten wires.

Diameter-nominal (mm)	Diameter-measured (mm)	Roughness-rms (μm)
0.38	0.3793	1.43
0.5	0.4965	1.78
0.75	0.7644	0.35
1	1.0105	3.65

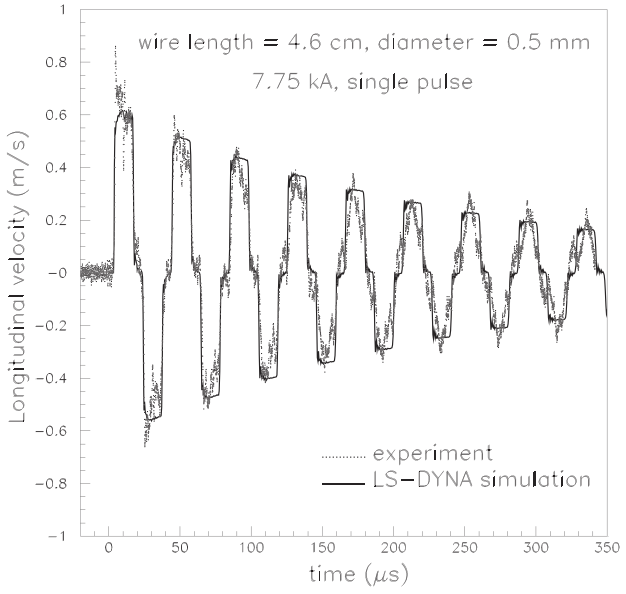

Fig. 3. Longitudinal velocity (dotted line-experiment; full line-simulation result [9]) of the 4.6 cm long tungsten wire as a function of time.

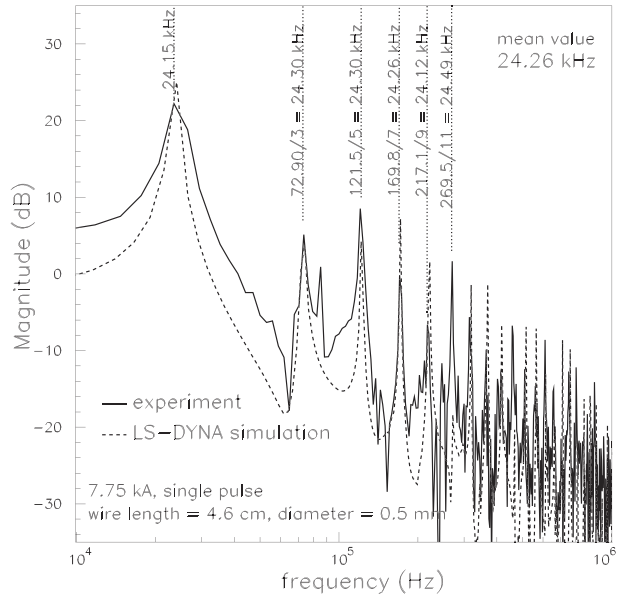

Fig. 4. Result of the FFT analysis of the wire longitudinal velocity shown in Fig. 3 and longitudinal velocity calculated by LS-DYNA [9].

Another feature of the experimental frequency spectrum in Fig. 4 is a spectral line at ~85 kHz which cannot be interpreted as a wire fundamental higher harmonic. The 85 kHz line, as well as other details which are not in full agreement with LS-DYNA results (dashed line), confirms that unknown parameters, such as a friction coefficient between the wire and graphite connectors, wire bending, etc., play an important role in this type of measurements. However, the main conclusion from these results is that it is possible to precisely measure Young's modulus using the LDV.

The measurement procedure has been repeated with a shorter, 3.9 cm long, wire with an expectation to get higher value of the fundamental frequency. This is exactly what was observed; the fundamental frequency of 3.9 cm long tungsten wire is $f_0 = (28.3 \pm 0.3)$ kHz which gives $E = (376 \pm 7)$ GPa.

Comparison between our results and the literature [11] is presented in Fig. 5. Our two results given above are denoted by filled circles in Fig. 5. The error bars result from the combined uncertainties in the measured frequency and wire dimension. Open circles show the measurement results obtained with a third, different wire by measuring longitudinal and radial oscillations at room temperature.

Fig. 6 (top) shows the radial displacement of the 0.5 mm diameter wire as a function of time and applied current. One can see that at $t = 0$ the wire starts to contract and then to expand and after ~1 μs it reaches a new equilibrium position and starts oscillating around it. Initial, relatively quick contraction of the wire is a result of the magnetic pressure effect.

Except for the fact that displacement increases with increasing current (as expected), one can see that high frequency oscillations are much more prominent for higher current values. This can be seen in Fig. 6 (bottom), together with almost perfect agreement between the measured frequency (6.85 MHz) and LS-DYNA prediction [9]. It should be noted that the frequency spectra obtained (including LS-DYNA result) lie on top of each other but they have been displaced vertically for clarity.

The measured radial frequency f can be used to extract the value of Young's modulus of tungsten using the formula [12]:

$$E = \frac{(2\pi f)^2 r^2 \rho}{\zeta^2} \cdot \frac{(1+\nu)(1-2\nu)}{(1-\nu)}, \tag{3}$$

where r is the wire radius, ρ is the density (see Eq. (2)) and ν is Poisson's ratio for tungsten which depends on temperature (in °C) in a following way:

$$\nu = 0.279 + 1.0893 \times 10^{-5} \cdot T. \tag{4}$$

$\zeta$is the root of the following Bessel function [12]:

$$\zeta J_0(\zeta) - \frac{(1-2\nu)}{(1-\nu)} J_1(\zeta) = 0, \tag{5}$$

and its dependence on Poisson's ratio, for $\nu < 0.5$, can be parametrized as:

$$\zeta = 1.8411 + 0.7852 \cdot \nu + 0.3317 \cdot \nu^2 + 0.704 \cdot \nu^3. \tag{6}$$

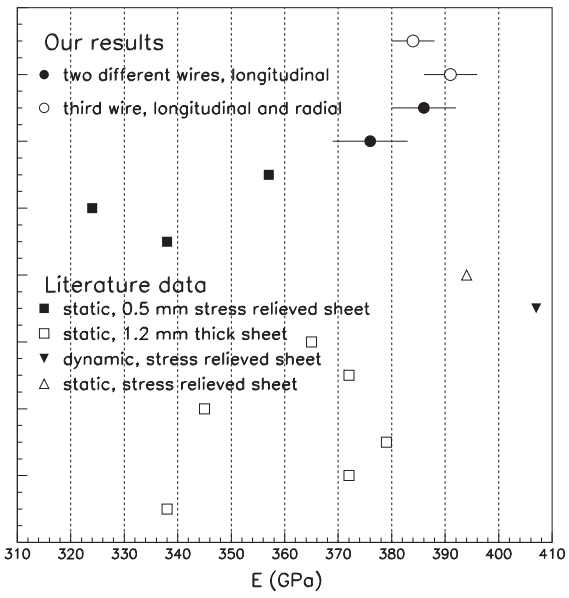

Fig. 5. Comparison between measured values of the Young's modulus of tungsten at room temperature and the literature [11].

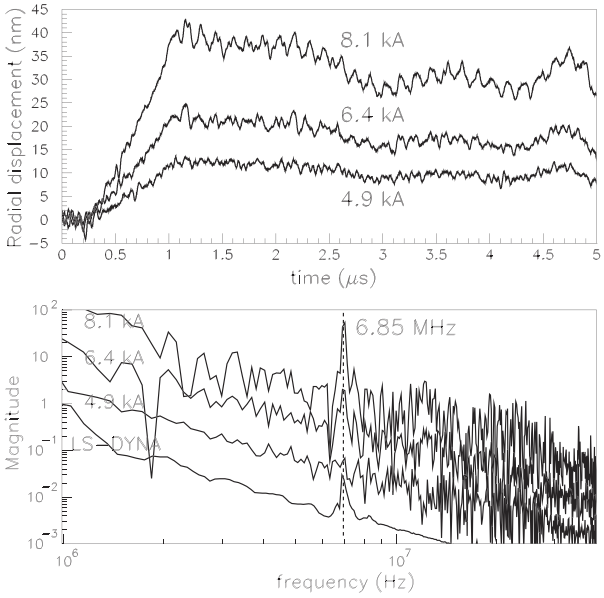

Fig. 6. (Top) Radial displacement of the 0.5 mm wire as a function of applied current. (Bottom) Corresponding frequency spectra.

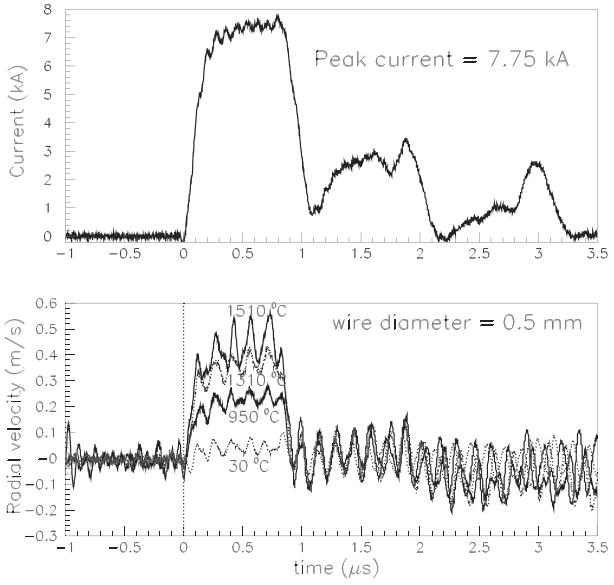

Fig. 7. (Top) The current pulse shape; (bottom) measured radial velocity of the 0.5 mm diameter tungsten wire as a function of time at different temperatures.

The measured value of Young's modulus of tungsten is shown as one of the open circles in Fig. 5. As can be seen, there is a full agreement between the results from radial and longitudinal measurements at room temperature. When discussing the literature data, it has to be noted that those measurements were usually performed with tungsten sheets and that the spread of results, even for the same group of samples, is quite large. In our case, however, the results lie in a relatively narrow region. Moreover, the agreement between the longitudinal and radial measurement results confirms that our methodology is consistent.

3.2. Young's modulus of tungsten at high temperature and stress

Only the measurements of radial wire oscillations have been used for the material characterization at high temperatures. This is because the longitudinal vibrations are the result of the non-homogeneous temperature distribution along the wire so it is difficult to say what the relevant temperature is. On the other hand, the radial vibrations are influenced only by the temperature jump occuring in the wire at the position where the LDV reading was taken. In addition, the longitudinal effects (including friction, bending, etc.) manifest themselves on a much longer time scale than the radial effects.

High temperature measurements are the most important goal of this study because this places the material sample under the conditions expected at the Neutrino Factory. A characteristic set of the high temperature results is shown in Fig. 7 and this reveals a number of interesting features:

- peak velocity rise with temperature;
- the visible change of frequency of wire vibrations as a function of temperature;
- the relatively small influence of current pulse "reflections" on wire motion and
- the relatively good signal/noise ratio.

For the two highest temperatures shown in Fig. 7, as the equivalent stress in the wire is equal to or larger than in the target at the Neutrino Factory (calculated to be ~300 MPa), the material properties are being measured under the exact conditions expected of a real target. Moreover, the almost perfect visibility of the high-frequency vibrations gives us a chance to precisely measure Young's modulus of tungsten under these extreme conditions. For the highest temperature shown in Fig. 7 the peak strain-rate is well above 1000 s^{-1}. An extensive set of measurements of the radial frequencies has been performed and using the formulae (2)–(4) and (6), the values of Young's moduli have been obtained over a wide range of temperatures.

Fig. 8 shows Young's modulus of a 0.5 mm diameter tungsten wire as a function of temperature for four different peak currents. One can see that the modulus of elasticity decreases with increasing temperature. More importantly, we can conclude that the behaviour of Young's modulus of tungsten does not depend on the induced stress.

Fig. 9 summarizes our results of tungsten Young's modulus dependence on temperature obtained by measuring characteristic frequency of radial vibration of 0.38, 0.5, 0.75 and 1 mm diameter

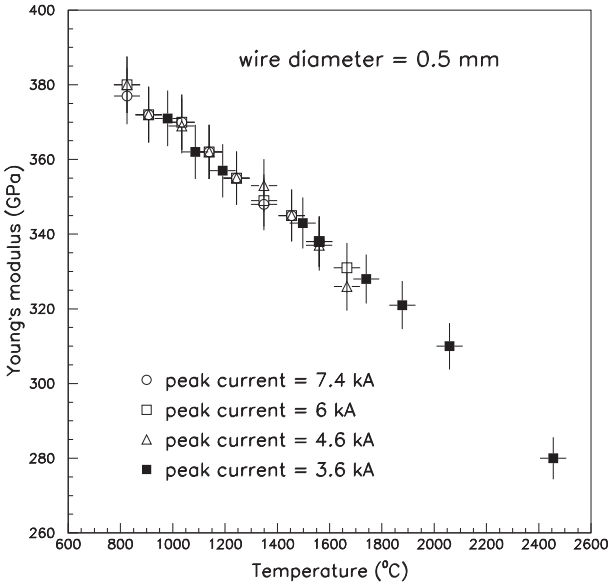

Fig. 8. Young's modulus of a 0.5 mm diameter tungsten wire as a function of temperature for four different peak currents.

tungsten wires. For the sake of completeness, we have also included room temperature data (single pulse test results) shown before in Fig. 6. The results for 0.38, 0.5 and 1 mm diameter samples agree very well.

The highest temperature has been reached with 0.75 mm diameter wire but this set of results lies below the other data. The maximum value of sample-to-sample difference is at the level of 10%, which is very small compared to the scatter seen with existing data. During these tests it has been observed that 0.75 mm diameter samples are much smoother than the others, which was confirmed by precise measurement of surface roughness (see Table 1). Further, the 0.75 mm diameter wires are not in a list of manufacturer's standard samples and they were made under special order. As a result, it is likely that these wires are manufactured differently. Despite this difference the measurements show that the Young's modulus of tungsten remains high at high temperatures and high stress.

A comparison between these measurements and a compilation of existing Young's modulus measurements is shown in Fig. 10. The difference compared to the static measurements arises because those in this paper are dynamic.

3.3. Young's modulus of tantalum at high temperature and stress

The procedure described in the previous sections has been used to measure Young's modulus of tantalum as a function of temperature and applied stress. As the tantalum is too weak to sustain prolonged stress at the magnitude observed in the tests with tungsten, the stress in this case is two times lower (on average) than in corresponding tungsten test, but still satisfying high stress and high-strain-rate conditions. Eq. (3) has been used, again, for the extraction of the Young's modulus, combining the measured value of fundamental radial frequency of the wire, the temperature-dependent parametrization of the density of tantalum:

$$\rho = 16.603 - 3.2592 \times 10^{-4} \cdot T - 2.019 \times 10^{-8} \cdot T^2, \quad (7)$$

where ρ is given in (g/cm^3) and temperature in (°C), the temperature-dependent parametrization of Poisson's ratio for tantalum:

$$\nu = 0.35 + 7.337 \times 10^{-6} \times T, \quad (8)$$

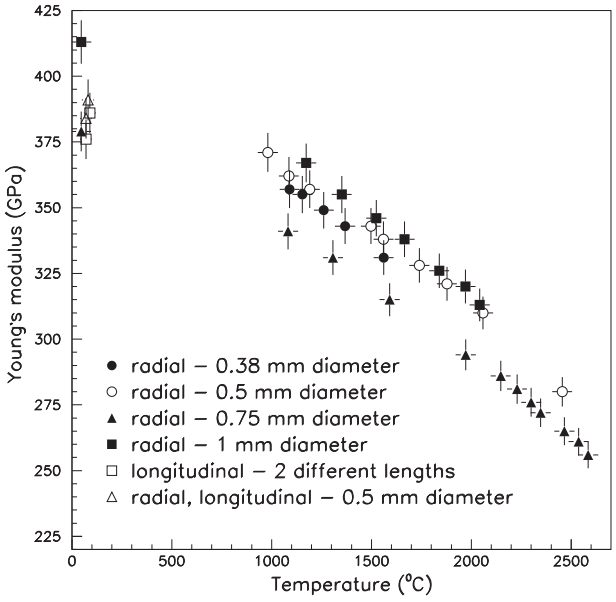

Fig. 9. Compilation of our experimental results on Young's modulus of tungsten as a function of temperature.

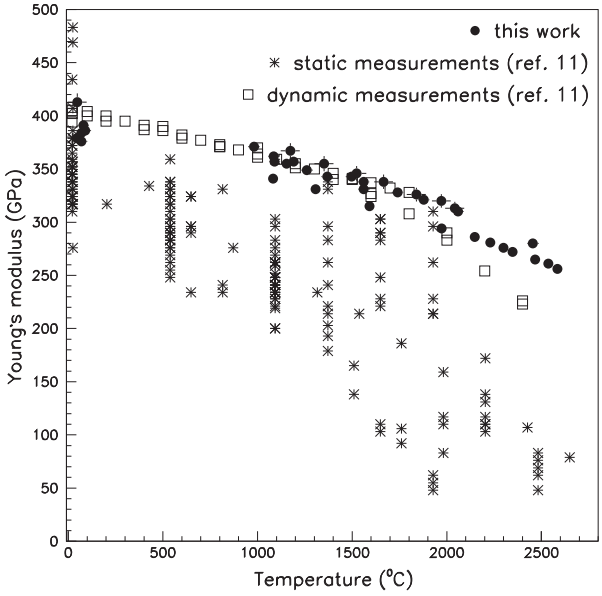

Fig. 10. Comparison between our experimental results and previous results [11] on tungsten Young's modulus.

and the root of the Bessel function (see Eq. (6)). Fig. 11 summarizes our results of the dependence of Young's modulus of tantalum on temperature obtained by measuring characteristic frequency of radial vibration of 0.5 and 0.8 mm diameter wires. The error bars result from the combined uncertainties in the measured frequency and wire dimension. These results for 0.5 and 0.8 mm diameter samples agree almost perfectly and the values of the parameters by fitting a polynomial function are shown in Fig. 11. As in the tungsten case, the behaviour of Young's modulus of tantalum does not depend on the induced stress.

4. Discussion

When discussing these results for Young's modulus as a function of temperature, it should be noted that they depend on a set of parameters that define the material behaviour (electrical con-

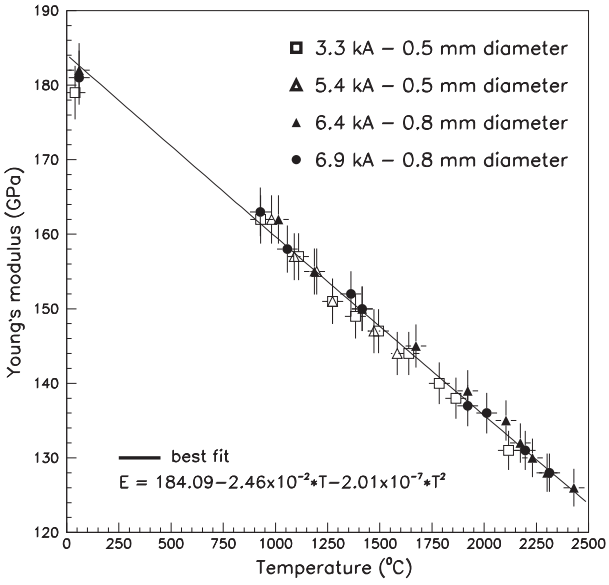

Fig. 11. Results of Young's modulus of tantalum as a function of temperature.

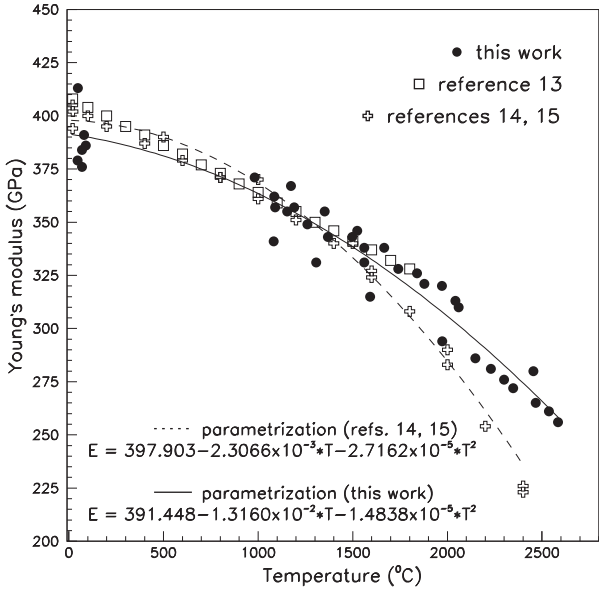

Fig. 12. Comparison between these experimental results and previous results of dynamic measurements [13–15] of Young's modulus for tungsten.

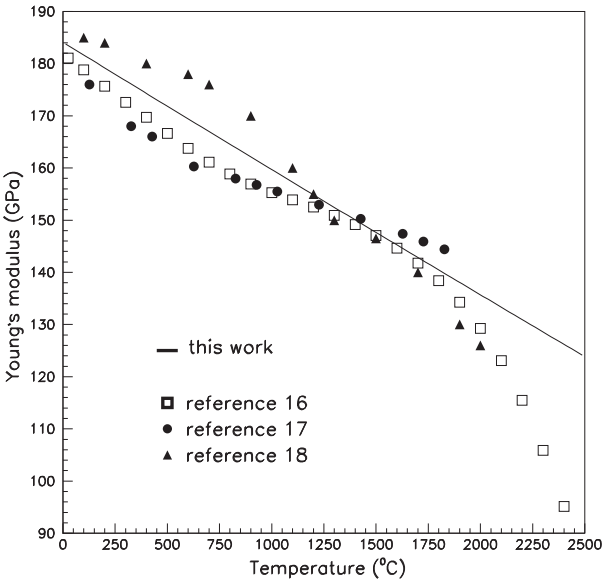

Fig. 13. Comparison between the new experimental data and previous results [16–18] on tantalum Young's modulus.

ductivity, coefficient of thermal expansion, etc.). All of these are temperature dependent. However, if we choose the characteristic frequency as a measured observable this multi-parameter phase space is reduced to only three degrees of freedom: Young's modulus, density and Poisson's ratio (see Eq. (3)). Poisson's ratio and density depend on temperature relatively weakly (see Eqs. (2) and (4) for tungsten and (7) and (8) for tantalum) and definitely more weakly than Young's modulus. The parametrizations of Poisson's ratio and density dependence on temperature have been used in LS-DYNA simulations and this resulted in a very good agreement with experimental results [9]. The measured value of Poisson's ratio at room temperature agrees very well with the expected value from Eq. (4).

The comparison between our measurements of temperature dependence of tungsten Young's modulus and previous dynamic (sonic) results is shown in Fig. 12. In [11] three sets of results [13–15] can be found and they have been used for this comparison. Results from [13] agree very well with those in this paper while there is a significant difference between the high temperature data (above 1800 °C) and results from references [14,15]. As mentioned in [11], these references did not indicate the method of testing but are believed to be dynamic measurements. A possible cause is that the measurements for this paper are made under high-strain rate conditions.

A similar conclusion can be drawn from the analysis of the Young's modulus results for tantalum. The comparison between the new and previous results [16–18] on the temperature dependence of Young's modulus is shown in Fig. 13. There is good agreement between all three sets of previous results with the new data up to 1800 °C. At higher temperatures there is a significant difference between the new results and the only existing set of data [16]. This again may be a result of high-strain rate conditions in this experiment.

The parametrizations of the temperature dependence of Young's modulus of tantalum and tungsten are shown as a full line in Figs. 11 and 12, respectively. In the tungsten case, the parametrization reads:

$$E = 391.448 - 1.3160 \times 10^{-2} \times T - 1.4838 \times 10^{-5} \times T^2, \quad (9)$$

where E is in (GPa) and T is given in (°C). This equation is recommended for use up to the temperature limit of the experimental data of 2650 °C, and especially in the case of relatively high-strain rates.

For tantalum, the recommended parametrization is:

$$E = 184.09 - 2.46 \times 10^{-2} \times T - 2.01 \times 10^{-7} \times T^2, \quad (10)$$

where E is in (GPa) and T is given in (°C), to be used up to 2500 °C.

5. Summary

An extensive set of measurements of the surface displacement and velocity of tungsten wires at high temperature and high stress has been performed. Stress is induced by passing a fast, high current pulse through a thin wire and the radial and longitudinal motion of the sample measured by a laser Doppler vibrometer. The wire is operated at temperatures of 300–2900 K by adjusting the pulse repetition rate. In doing so, simulation of the conditions (high stress and temperature) expected at the Neutrino Factory has been reached. Measurements of the characteristic frequencies of surface oscillations have been used to obtain the moduli of elasticity of tungsten and tantalum as a function of temperature and stress. It has been found that Young's modulus does not depend on the level of induced shock and that the new results agree very well with previous results up to 1800 °C. At very high temperatures, the new data lie higher than some literature data but this might be explained as a result of high-strain rate conditions in the experiment.

References

[1] International Scoping Study of a Future Neutrino Factory and Super-beam Facility, Physics at a Neutrino Factory and Super-beam Facility, arXiv:0710.4947v2 [hep-ph], November 2007.
[2] J.R.J. Bennett et al., Journal of Nuclear Materials 377 (1) (2008) 285–289.
[3] T.R. Edgecock et al., in: Proceedings of IPAC'10, Kyoto, Japan, THPEC089, 2010, pp. 4263–4265.
[4] Livermore Soft. Techn. Corp. <http://www.lstc.com/>.
[5] J.R. Barber, Elasticity, third ed., Springer, Dordrecht, 2010.
[6] The ISIS web site: <http://www.isis.rl.ac.uk/>.
[7] Polytec web site.: <http://www.polytec.com>.
[8] J.W. Davis, V. Barabash, ITER Material Properties Handbook AM01-3111 (3) (1997) 1–4.
[9] G.P. Škoro et al., in: Proceedings of IPAC'10, Kyoto, Japan, THPEC091, 2010, pp. 4269–4271.
[10] http://www.mathworks.com/products/matlab/.
[11] J.W. Davis, ITER Material Properties Handbook AM01-2111 (2) (1997) 1–7.

[12] J.R. Airey, Arch. d. Math. u. Phys. 20 (3) (1913) 289–294.
[13] Metals Handbook, 9th Edition, Vol. 2, Properties ans Selection: Nonferrous Alloys and Pure Metals, American Society for Metals, Metals Park, Ohio, 1979.
[14] Properties of Elements, in: G.V. Samsonov (Ed.), Moscow, Metallurgy, 1976 (in Russian).
[15] L.V. Tikhonov et al., Structure and Properties of Metals and Alloys, Naukova Dumka, Kiev, 1986.
[16] P.A. Armstrong, H.L. Brown, Trans. AIME 230 (1964) 962.
[17] R. Farraro, R.B. McLellan, Metall. Trans. 10A (1979) 1699.
[18] T.E. Tietz, J.W. Wilson, Behavior and Properties of Refractory Metals, Stanford University Press, Stanford, CA, 1965.